

RESEARCH ARTICLE

Differential reaction norms to ocean acidification in two oyster species from contrasting habitats

Coline Caillon¹, Fabrice Pernet¹, Mathieu Lutier^{1,2} and Carole Di Poi^{1,*}

ABSTRACT

Ocean acidification (OA), a consequence of the increase in anthropogenic emissions of carbon dioxide, causes major changes in the chemistry of carbonates in the ocean with deleterious effects on calcifying organisms. The pH/ P_{CO_2} range to which species are exposed in nature is important to consider when interpreting the response of coastal organisms to OA. In this context, emerging approaches, which assess the reaction norms of organisms to a wide pH gradient, are improving our understanding of tolerance thresholds and acclimation potential to OA. In this study, we deciphered the reaction norms of two oyster species living in contrasting habitats: the intertidal oyster *Crassostrea gigas* and the subtidal flat oyster *Ostrea edulis*, which are two economically and ecologically valuable species in temperate ecosystems. Six-month-old oysters of each species were exposed in common garden tanks for 48 days to a pH gradient ranging from 7.7 to 6.4 (total scale). Both species were tolerant down to a pH of 6.6 with high plasticity in fitness-related traits such as survival and growth. However, oysters underwent remodelling of membrane fatty acids to cope with decreasing pH along with shell bleaching impairing shell integrity and consequently animal fitness. Finally, our work revealed species-specific physiological responses and highlights that intertidal *C. gigas* seem to have a better acclimation potential to rapid and extreme OA changes than *O. edulis*. Overall, our study provides important data about the phenotypic plasticity and its limits in two oyster species, which is essential for assessing the challenges posed to marine organisms by OA.

KEY WORDS: Bleaching, Fatty acid, Mollusc, pH, Plasticity, Tipping point

INTRODUCTION

The increase in atmospheric CO_2 emissions since the Industrial Revolution and its subsequent uptake by the ocean have led to an imbalance in seawater carbonate chemistry, causing a decrease in pH, a process known as ocean acidification (OA) (Caldeira and Wickett, 2003). The most likely climate model predicts that sea-surface pH will decrease by 0.032 pH units by the end of the century (SSP3-7.0; IPCC, 2022). Concomitantly, the excess of hydrogen ions (H^+) is responsible for a reduction in the availability of

carbonate ions (CO_3^{2-}), the essential components of the shells and skeletons of marine calcifiers (Orr et al., 2005).

In most experimental studies, marine organisms are exposed to constant acidification levels derived from the IPCC OA scenarios for the global ocean, while most of them inhabit variable coastal environments such as intertidal, estuarine and upwelling areas (Cai et al., 2011; Feely et al., 2008; Provoost et al., 2010). In these habitats, current seawater pH/ P_{CO_2} levels vary more temporally and spatially than in the open ocean, and may already exceed average OA projections (Vargas et al., 2017). Therefore, this large environmental variability in combination with expected global future acidification could drive resident organisms even closer to the limits of their physiological tolerance (Hofmann et al., 2011). To address this constraint, a few studies have investigated the physiological tolerance and acclimation capacities of coastal organisms to OA by assessing reaction norms to a broad range of pH levels, covering the natural variability of seawater chemistry (Comeau et al., 2013; Dorey et al., 2013; Lutier et al., 2022; Thor et al., 2018; Ventura et al., 2016). In addition, reaction norms can be used to identify physiological tipping points, corresponding to tolerance thresholds beyond which a small change in an environmental factor has large effects on the organism (Scheffer, 2010). Such approaches have proven to be complementary methods to standard scenario studies (present-day versus future), but they need to consider the entire natural pH/ P_{CO_2} range to which species are exposed to be relevant (Vargas et al., 2017).


Among coastal organisms, shelled molluscs are considered particularly vulnerable to OA as acidified conditions lead to a decrease in the calcite and aragonite saturation states, which adversely affects their calcification, shell integrity and survival (Gazeau et al., 2013; Waldbusser et al., 2015). Nevertheless, it is worth noting that there are species- and population-specific responses to OA that can be explained by divergent selection and plasticity, which may or may not allow a set of organisms to cope with rapid and extreme acidification events (Duarte et al., 2015; Parker et al., 2010). Interestingly, molluscs living in environments with high natural pH/ P_{CO_2} variability seem less sensitive to OA (Thomsen et al., 2017; Vargas et al., 2017; 2022), and intertidal organisms seem to have evolved greater tolerance to lower pH than their subtidal counterparts (Leung et al., 2017; Scanes et al., 2017).

Here, we aimed to determine and compare the reaction norms to OA of two economically and ecologically valuable oyster species living at different bathymetric levels. The Pacific oyster *Crassostrea gigas* (Thunberg 1793) is distributed worldwide and predominantly inhabits the upper intertidal zone where it can experience severe metabolic hypercapnia during emersion (Burnett, 1988; Zwerschke et al., 2018). Indeed, intertidal oysters are exposed to spatially and temporally heterogeneous environments in terms of temperature, pH, oxygen, salinity and food supply conditions, throughout the tidal cycle, leading to extended phenotypic plasticity (Chevin and Hoffmann, 2017; Leeuwis and Gamperl, 2022). In contrast, the flat

¹Ifremer, Univ Brest, CNRS, IRD, UMR 6539 LEMAR, 29280 Plouzané, France.

²Section for Aquatic Biology and Toxicology, Department of Biosciences, University of Oslo, Blindernveien 31, 0371 Oslo, Norway.

*Author for correspondence (carole.dipoi@ifremer.fr)

 C.C., 0009-0000-7012-2386; F.P., 0000-0001-8886-0184; M.L., 0000-0003-3955-9277; C.D., 0000-0001-7846-5287

oyster *Ostrea edulis* Linnaeus 1758 is found only in Europe and lives mainly in the more stable subtidal zones where it rarely or never emerges (Pogoda, 2019; Laing et al., 2006). The life history traits of the two species are very different, with *C. gigas* reproducing through broadcast spawning and *O. edulis* using a brooding strategy, which can also lead to contrasting responses to changing environments (Gray et al., 2019; Stechele et al., 2022).

We therefore hypothesised that the reaction norms of the two oyster species to OA would differ, and that the intertidal *C. gigas* may be more tolerant to pH decrease than its subtidal counterpart *O. edulis*. To test our hypothesis, we established their reaction norms over a wide pH range, from 7.7 to 6.4, under laboratory conditions. We investigated the effect of decreasing pH on macrophysiological traits such as survival, growth and shell coloration. Indeed, acidification bleaches shells and the coloration is a simple and reliable indicator of the acidity of water and its impact on the integrity of molluscs' shells (Avignon et al., 2020). We also measured the energy reserves of oysters as a function of pH. Acclimation to acidification generally involves energy reallocation and strategies may differ depending on the species (Sokolova, 2013). Finally, we analysed the composition of membrane fatty acids, a key parameter governing exchanges between intracellular and extracellular compartments and overall metabolic rates (Hulbert, 2003). Overall, our study provides insight into phenotypic plasticity divergence in two oyster species from contrasting habitats, and a better understanding of how oysters are likely to respond and acclimatise in a rapidly acidifying ocean.

MATERIALS AND METHODS

Animals and maintenance

Because of the different reproduction strategies between the two oyster species studied, the production and fertilisation protocols used were different. Pacific oysters were produced at the Ifremer experimental station (Argenton, Brittany, France) on 27 August 2019, according to the procedure described in Petton et al. (2015). Briefly, the broodstock consisted of 118 females and 22 males collected in the natural environment between 2011 and 2017 in Île d'Aix (Charente-Maritime, France; 46°00'40.8"N, 1°09'39.4"W), whose gametes were obtained by stripping and mixed in the same jar to fertilise the oocytes. At 1 month old, the juvenile oysters were transferred dry in a cooler to the Ifremer station in Bouin (Vendée, France) for growing in a flow-through seawater system depending on the temperature and pH of the natural environment. During this phase, the animals were fed a monospecific diet *ad libitum* with the microalga *Skeletonema costatum* (strain CCAP 1077/3). On 9 January 2020, these oysters were brought back to the Argenton facilities and kept in a 500 l flow-through tank for 19 days before the experiment.

In the flat oyster, the fertilisation is internal and the females incubate the larvae for nearly 10 days in the paleal cavity. Compared with that of the Pacific oyster, hatchery culture of the flat oyster is delicate and mortality occurs depending on feeding and water flow regimes (Maneiro et al., 2020). We used juvenile oysters obtained by biparental mating (paired crossing) at the hatchery of the Comité Régional de la Conchyliculture (Lampaul-Plouarzel, Brittany, France) on 19 August 2019. The two parents used for breeding were wild oysters collected in the Bay of Brest by a professional hatchery (48°22'37.0"N, 4°25'29.1" W) in May 2019. On 17 January 2020, the juvenile oysters were transferred to the Argenton facilities and kept for 11 days in the same flow-through tank as the Pacific oysters.

During this time, the seawater temperature was gradually increased from 14°C to 19°C (+0.5°C day⁻¹), which is an optimal temperature for both species (Bayne, 2017). Salinity and pH were on

average 34.7±0.1 and 8.0±0.0, respectively. Oysters were continuously fed a mixed diet of two phytoplankton species (1:1 dry weight), the diatom *Chaetoceros muelleri* (8–10 µm diameter; strain CCAP 1010/3) and the haptophyte *Tisochrysis lutea* (4–5 µm diameter; strain CCAP 927/14). Phytoplankton concentration was maintained at 1500 µm³ µl⁻¹ at the tank outlet to ensure *ad libitum* feeding (Petton et al., 2015), and monitored twice daily using an electronic particle counter (Multisizer 3, Beckman Coulter, Indianapolis, IN, USA; 100 µm aperture tube). On 28 January 2020, at the onset of the experiment, the mean individual shell length and total mass were 18.5±3.0 mm and 0.67±0.18 g for *C. gigas*, and 8.9±2.1 mm and 0.10±0.08 g for *O. edulis*. Both species were divided into 16 batches each containing 105±3 and 105±4 individuals of *C. gigas* and *O. edulis*, respectively, for a total biomass of 91.9±2.4 g.

Experimental design

Each batch of oysters was exposed in 'common garden' tanks, i.e. both oyster species were maintained together in the same tank, to one constant nominal total pH (pH_T) condition ranging from pH 7.9 to 6.4, without pH replication, with a step of 0.1 between two levels, at 19°C for 48 days and fed *ad libitum* as described above. The experimental flow-through system consisted of 17 experimental units that were randomly assigned to one pH condition (*n*=16) or to a control blank without animals (*n*=1) to check the pH of the ambient seawater. Each experimental unit consisted of a header tank in which seawater was acidified by injecting pure CO₂ (except for the ambient pH condition) and then delivered by a pump (ProFlow t500, JBL, Neuhofen, Germany) to a holding tank containing the oysters. These tanks were 45 l and their entire volume was renewed every 90 min.

The pH level was controlled in the header tank using a pH controller connected to a pH electrode (ProFlora, JBL). The pH electrode was calibrated with NBS (National Bureau of Standards) buffers (pH 4.00 and 7.00) at the beginning of the experiment. In the holding tank, the seawater was continuously oxygenated and mixed using air bubbling and a circulation pump (ProFlow t300, JBL). The tanks were emptied and both tanks and oysters were rinsed with freshwater twice a week. The photoperiod was fixed at 14 h light:10 h dark and no tidal regime was applied. Seawater was sampled twice daily at the inlet and outlet of each holding tank to determine the phytoplankton concentration (in cell volume) and total consumption of both species simultaneously using the electronic particle counter. When needed in each pH condition, the phytoplankton concentration at the inlet was gradually increased over time to compensate for the increasing grazing rate of the growing oysters (Fig. S1). Considering the seawater renewal time of the tanks, pH had no effect on the quality of microalgae (Fig. S2).

Seawater carbonate chemistry

Seawater pH_T, temperature, dissolved oxygen saturation and salinity were monitored twice daily in the holding tanks using a portable multi-parameter device (MultiLine® Multi 3630 IDS – WTW: pH electrode SenTix® 940, oxygen sensor FDO® 925, conductivity electrode TetraCon® 925, Xylem Analytics, Weilheim in Oberbayern, Germany). These measurements were used to adjust the settings of the pH controllers. The accuracy of the pH electrode was checked once a week with Certipur® NBS buffers (pH 4.00, 7.00 and 9.00; Merck, Darmstadt, Germany) and calibrated twice a week on the total scale (pH_T) with a certified Tris/HCl buffer at a salinity of 35.0 (provided by A. G. Dickson, Scripps Institution of Oceanography, San Diego, CA, USA). Seawater samples (150 ml)

were collected three times during the experiment for total alkalinity (A_T) analyses. The seawater was filtered through 0.7 μm GF/F glass microfiber filters (Whatman®, Florham Park, NJ, USA) and immediately poisoned with 0.05% saturated mercuric chloride solution before storage. A_T was measured at the Laboratoire Environnement Ressources (Sète, Hérault, France) using potentiometric titrations with an automatic titrator (TitroLine® 7000; SI Analytics, Mainz, Germany) according to Dickson et al. (2007). A_T measurements were conducted in triplicate at 20°C on 25 ml subsamples with a measurement uncertainty of 0.44%. Parameters of the carbonate system were determined from pH_T , A_T , temperature and salinity using the R package *seacarb* (v3.3.1; <https://CRAN.R-project.org/package=seacarb>) (see Table 1).

Oyster survival

For each species, oyster survival was assessed visually inside the tanks once a day, then more exhaustively twice a week during cleaning. The dead individuals were immediately removed.

Biometric measurements

Total body mass (shell+tissue), and both shell length and mass, were measured individually with a calliper (Digimatic IP67, Mitutoyo, Sakado, Japan) and a precision balance (Mettler-Toledo, Greifensee, Switzerland) on a subsample of 30 individuals of each species at the start of the experiment (day 0), and on 20 oysters per species and pH condition after 41 days of exposure. The dissected flesh was pooled and weighted to obtain fresh flesh mass. Growth rate (G) was calculated as:

$$G = \frac{\overline{X}_{41} - \overline{X}_0}{41}, \quad (1)$$

where G is the growth rate expressed as an increase in shell length or total body mass per day (mm day^{-1} and mg day^{-1} , respectively), and \overline{X}_0 and \overline{X}_{41} are the mean values measured at the onset of the experiment (day 0) and at 41 days. The measurements relate to different individuals between day 0 and day 41.

Shell coloration

Analysis of shell coloration was performed on day 20, as shell condition deteriorated under the lowest pH conditions afterwards. The digestive gland was apparent through the shell later in the exposure and could distort shell coloration measurements. Fifteen individuals per species and pH condition were randomly selected. Their left valves were photographed using an ultra-high precision digital microscope (Keyence® VHX-5000, Keyence Corporation, Osaka, Japan). The images were converted into grayscale images and analysed using ImageJ software (<https://imagej.net/ij/index.html>). The mean coloration of the shell was calculated using the mean value of the grey levels of all pixels constituting the selected area (Fig. 1). Grayscale level was measured on a scale of 0 to 255 where 0 is black and 255 is white.

Biochemical analyses

Soft-tissue samples from 10 individuals per species and pH condition were collected at day 41, flash-frozen under liquid nitrogen, pooled, ground to a powder with a ball mill and stored at -80°C until analyses. Lipids and carbohydrates were not analysed for flat oysters exposed to pH below 6.8 and 6.9, respectively, because of the low amount of flesh available.

Energy reserves

Oyster powder was diluted with chloroform/methanol (2:1, v/v) and the neutral lipids (i.e. reserve lipids) were separated into lipid classes and quantified using a high-performance thin-layer chromatography and a scanning densitometer (Automatic TLC Sampler 4 and TLC Scanner 3, respectively, CAMAG, Muttenz, Switzerland). As triacylglycerols (TAG) are mainly reserve lipids and sterols (ST) are structural lipids of cell membranes, the TAG:ST ratio was used as an index for the contribution of energy reserves to structure (Fraser, 1989).

The carbohydrate content was determined according to the colorimetric method described in Dubois et al. (1956). Milli-Q water was added to the powder samples and mixed with phenol (0.5 ml, 5% m/v) and sulphuric acid (2.5 ml, 98%), and then incubated for 40 min. Absorbance was measured at 490 nm using a

Table 1. Parameters of seawater carbonate chemistry in each experimental tank (16 pH_T levels and a blank without oysters)

| Nominal pH | Measured | | | | Calculated | | | | |
|------------|---------------|-----------------------------------|--------------------------|-----------|------------|---------------------------------------|---------------------------------|------------|------------|
| | pH_T | A_T ($\mu\text{mol kg}^{-1}$) | T ($^\circ\text{C}$) | S (PSU) | DO (%) | P_{CO_2} (μatm) | DIC ($\mu\text{mol kg}^{-1}$) | Ω_C | Ω_A |
| Blank | 7.9±0.0 | 2444±6 | 19.1±0.1 | 34.6±0.2 | 100.4±0.5 | 693±22 | 2275±8 | 3.2±0.1 | 2.1±0.0 |
| 7.9 | 7.7±0.0 | 2349±29 | 19.1±0.1 | 34.6±0.2 | 98.7±0.7 | 947±18 | 2239±23 | 2.3±0.1 | 1.5±0.1 |
| 7.8 | 7.7±0.0 | 2350±54 | 19.2±0.1 | 34.6±0.2 | 98.6±0.6 | 964±54 | 2242±44 | 2.3±0.2 | 1.5±0.1 |
| 7.7 | 7.7±0.0 | 2321±37 | 19.2±0.1 | 34.6±0.2 | 98.5±0.7 | 1085±51 | 2233±39 | 2.0±0.0 | 1.3±0.0 |
| 7.6 | 7.6±0.1 | 2339±57 | 19.1±0.1 | 34.6±0.2 | 97.7±0.9 | 1382±312 | 2281±79 | 1.7±0.3 | 1.1±0.2 |
| 7.5 | 7.5±0.0 | 2345±27 | 19.1±0.1 | 34.6±0.2 | 98.6±0.6 | 1814±59 | 2325±29 | 1.3±0.0 | 0.9±0.0 |
| 7.4 | 7.4±0.0 | 2368±55 | 19.1±0.1 | 34.6±0.2 | 98.4±0.7 | 2292±126 | 2378±57 | 1.1±0.0 | 0.7±0.0 |
| 7.3 | 7.3±0.0 | 2361±29 | 19.1±0.1 | 34.6±0.2 | 98.1±0.9 | 2901±575 | 2403±55 | 0.9±0.1 | 0.6±0.1 |
| 7.2 | 7.2±0.0 | 2369±28 | 19.1±0.1 | 34.6±0.2 | 98.2±0.7 | 3405±153 | 2436±22 | 0.8±0.0 | 0.5±0.0 |
| 7.1 | 7.1±0.0 | 2391±33 | 19.2±0.1 | 34.6±0.2 | 98.8±0.6 | 4578±125 | 2508±37 | 0.6±0.0 | 0.4±0.0 |
| 7.0 | 7.0±0.0 | 2412±60 | 19.2±0.1 | 34.6±0.2 | 98.7±0.6 | 5759±152 | 2574±59 | 0.5±0.0 | 0.3±0.0 |
| 6.9 | 6.9±0.1 | 2404±22 | 19.1±0.1 | 34.6±0.2 | 98.8±0.5 | 6808±476 | 2606±4 | 0.4±0.0 | 0.3±0.0 |
| 6.8 | 6.8±0.1 | 2426±20 | 19.2±0.1 | 34.6±0.2 | 99.2±0.4 | 9655±1173 | 2728±59 | 0.3±0.0 | 0.2±0.0 |
| 6.7 | 6.7±0.1 | 2433±21 | 19.1±0.1 | 34.6±0.2 | 99.0±0.5 | 10,482±631 | 2765±23 | 0.3±0.0 | 0.2±0.0 |
| 6.6 | 6.6±0.0 | 2445±15 | 19.2±0.1 | 34.6±0.2 | 99.1±0.4 | 15,930±2494 | 2962±93 | 0.2±0.0 | 0.1±0.0 |
| 6.5 | 6.5±0.1 | 2458±23 | 19.1±0.1 | 34.6±0.2 | 98.9±0.6 | 20,108±1915 | 3117±70 | 0.1±0.0 | 0.1±0.0 |
| 6.4 | 6.4±0.0 | 2453±24 | 19.1±0.1 | 34.6±0.2 | 98.7±0.6 | 22,186±1493 | 3182±72 | 0.1±0.0 | 0.1±0.0 |

Seawater pH on the total scale (pH_T), temperature (T), dissolved oxygen saturation (DO) and salinity (S) were measured twice daily and averaged over the entire experimental period, while total alkalinity (A_T) was measured three times over the experiment. Partial pressure of CO_2 (P_{CO_2}), dissolved inorganic carbon concentration (DIC), and the saturation state of calcite (Ω_C) and aragonite (Ω_A) were calculated from pH_T , A_T , S and T using the R package *seacarb* (<https://CRAN.R-project.org/package=seacarb>). Values correspond to means±s.d.

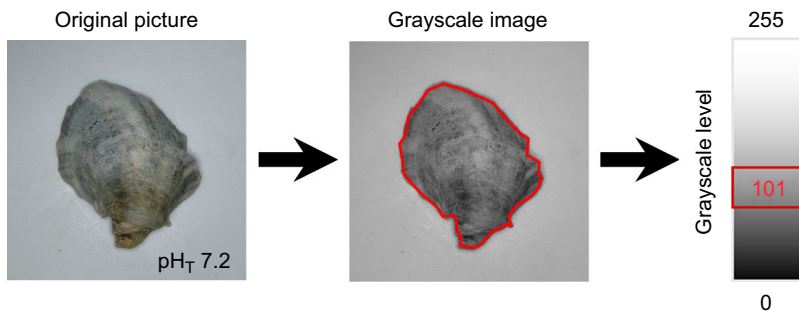


Fig. 1. Schematic representation of the procedure for analysing the coloration of oyster shells. The shell coloration was determined using ImageJ software that calculated the mean grayscale level of the entire left shell valve ranging from 0 (total black) to 255 (total white). pH_T , total pH.

Cary 60 UV-Vis spectrophotometer (Agilent Technologies, Santa Clara, CA, USA). Total carbohydrate content was calculated using a standard calibration curve with pure glucose and expressed in mg g^{-1} fresh mass.

Proteins were extracted from powder on ice using lysis buffer [150 mmol l^{-1} NaCl (Merck), 10 mmol l^{-1} Tris/HCl (Sigma-Aldrich), 1 mmol l^{-1} EDTA (Quantum), 1 mmol l^{-1} EGTA (Sigma-Aldrich), 1% Triton X-100 (Bio-Rad) and 0.5% Igepal (Sigma-Aldrich); pH 7.4 at 4°C] with phosphatase and protease inhibitors [1% of phosphatase inhibitor cocktail II (Sigma-Aldrich), 2% NaPPi 250 mmol l^{-1} (Sigma-Aldrich), and a tablet of complete EDTA free protease inhibitor cocktail (Roche) in 25 ml of lysis buffer]. Samples were ground and homogenised using a Polytron® PT 2500 E (Kinematica, Malters, Switzerland). The resulting lysates were used for quantification of the total protein content with the DC protein assay (Bio-Rad, Hercules, CA, USA) according to Lowry et al. (1951). Absorbance was read at 750 nm and protein concentrations were determined by comparison with a standard calibration curve supplied with the kit. The results were expressed as mg g^{-1} fresh mass.

Fatty acid composition of polar lipids

Polar lipids (i.e. membrane lipids) were purified from the chloroform/methanol mixture used for lipid class analysis on a silica-gel micro-column, and transesterified with a mixture of 3.4% sulphuric acid (H_2SO_4) in methanol at 100°C (Couturier et al., 2020). This transesterification produces fatty acid methyl esters (FAME) from the fatty acids, and dimethyl acetals (DMA) from the alkenyl chains at the sn-1 position of plasmalogens. The resulting FAME and DMA were analysed using a flame ionization detector gas chromatograph system (HP - Agilent 6890, Agilent Technologies, Santa Clara, CA, USA) equipped with a DB-Wax capillary column (30 m length \times 0.25 mm i.d. \times 0.25 μm film thickness). The DMA quantification allowed the indirect quantification of plasmalogens. Fatty acids were then identified by comparison of retention times with standards. Each fatty acid was expressed as the relative percentage of peak area by the sum of all polar fatty acid peaks.

Statistical analyses

All statistical analyses were performed using R software (v4.2.2; www.r-project.org/) and the significance threshold was set at 0.05. All variables were plotted using the mean pH_T calculated from daily measurements throughout the experiment in each pH condition. The general statistical procedure was previously described in Lutier et al. (2022).

The relationships between dependent variables (survival rate, biometrics, shell coloration, biochemistry) and the mean pH_T were computed using regression models. Segmented and linear regression models were tested and compared for each variable.

The model with the lowest Akaike and Bayesian information criteria (AIC, BIC) and the highest R^2 was selected. For segmented regression models, both the tipping point and its 95% confidence interval were estimated. The tipping point corresponds to the pH value at which the dependent variable tips, and was defined by applying the bootstrap restarting algorithm (Wood, 2001). For the growth rates, the critical point, i.e. the pH value at which the dependent variable was zero, and its 95% confidence interval were also determined. The normality of residuals and homogeneity of variances were graphically checked. The significance of each slope was tested using the Student *t*-test and compared with a horizontal slope of zero. The segmented regression models were computed using the *segmented* package (v1.6-2). Dependent variables were averaged over the number of individuals collected for each species and pH condition.

In addition, slopes of each regression model obtained for *C. gigas* and *O. edulis* were compared using the Welch two-sample *t*-test to detect significant differences in response to acidification between the two species. The comparison of slopes was carried out above and below the tipping point when one of the species' reaction norms had been modelled by a segmented model. The test was not performed if the slopes were not different from zero. The statistical outputs are summarised in Table 2.

Specifically, survival of both species was evaluated by the Kaplan–Meier (KM) method (Kaplan and Meier, 1958) for each pH condition. Survival time was measured in days from the onset of the experiment. KM survival curves were generated using the *survival* package (v3.5-5). Multiple pairwise comparisons were then made using the log-rank survival test to identify significant differences in survival between the different pH conditions. Final survival rates were extracted and tested against pH_T .

Fatty acid data were summarised using principal component analysis (PCA) for each species separately. Only fatty acid contributing to $>1\%$ were considered. The pH condition 7.5 for *C. gigas* was removed from the fatty acid data analysis because of extraction problems. The fatty acids were then divided into two groups according to their positive or negative correlation with the first principal component (PC1). The contribution of fatty acids (%) was then summed for each group and plotted as a function of pH_T .

RESULTS

pH regulation and carbonate chemistry

During the experiment, pH levels in the oyster tanks were stable and reached the targeted values, except for the highest pH conditions, which were both 7.7 instead of 7.8 and 7.9 (Table 1). This was probably due to oyster respiration, which lowered the pH of the incoming seawater (already at a pH_T of 7.9), despite a relatively high turnover rate of seawater relative to oyster biomass. Nevertheless, a seawater pH of 7.7 is already experienced by marine organisms in the natural environment (high-frequency data from CocoriCO₂

Table 2. Comparison of the reaction norms for whole-body and shell-related parameters in *Crassostrea gigas* and *Ostrea edulis* in response to ocean acidification

| Variable | Species | Model results | | Slope value | | Slope comparison | |
|----------------------|------------------|---------------|-----------|-------------|-------------|------------------|------------------|
| | | Regression | TP | <TP | >TP | <TP | >TP |
| Shell length | <i>C. gigas</i> | Segmented | 7.20±0.28 | 16.97±1.93 | 6.64±2.41 | <0.001 | 0.32 |
| | <i>O. edulis</i> | Linear | n.a. | | 7.55±0.61 | | |
| Total body mass | <i>C. gigas</i> | Linear | n.a. | | 2.29±0.14 | <0.001 | |
| | <i>O. edulis</i> | Linear | n.a. | | 0.50±0.04 | | |
| Shell mass | <i>C. gigas</i> | Linear | n.a. | | 1.55±0.09 | <0.001 | |
| | <i>O. edulis</i> | Linear | n.a. | | 0.40±0.03 | | |
| Flesh mass | <i>C. gigas</i> | Segmented | 7.16±0.26 | 0.55±0.06 | 0.21±0.07 | <0.001 | 0.001 |
| | <i>O. edulis</i> | Linear | n.a. | | 0.07±0.01 | | |
| Growth rate (length) | <i>C. gigas</i> | Segmented | 7.20±0.28 | 0.41±0.05 | 0.16±0.06 | <0.001 | 0.32 |
| | <i>O. edulis</i> | Linear | n.a. | | 0.18±0.01 | | |
| Growth rate (weight) | <i>C. gigas</i> | Linear | n.a. | | 55.85±3.39 | <0.001 | |
| | <i>O. edulis</i> | Linear | n.a. | | 12.16±0.98 | | |
| Shell coloration | <i>C. gigas</i> | Linear | n.a. | | -32.57±4.13 | n.a. | <0.001 |
| | <i>O. edulis</i> | Segmented | 6.93±0.25 | n.s. | -44.77±7.44 | | |

Comparison of the slopes was performed above (>TP) and below (<TP) the tipping point (TP) when one of the species displayed a segmented model. The test was not performed on slopes not significantly different from a zero horizontal slope. Values are TP or slope coefficient and their 95% confidence interval. Welch two-sample *t*-test was performed to compare species slopes and significant *P*-values (*P*<0.05) are indicated in bold. n.a., not applicable; n.s., not significant.

project: <https://cocorico2.ifremer.fr/en/Donnees>). A_T varied from 2321 to 2458 $\mu\text{mol kg}^{-1}$ and increased significantly with decreasing pH_T (*t*-test, *P*<0.001, $R^2=0.95$) until reaching control values (seawater with no oyster). Seawater was undersaturated ($\Omega < 1$) with respect to aragonite and calcite from pH levels 7.5 and 7.3, respectively.

Low pH induces oyster mortality particularly for *O. edulis*

No mortality was observed in *C. gigas* throughout the exposure period, except at the lowest pH_T of 6.4 where mortalities started at day 38 and survival dropped to 78% at the end of the experiment (Fig. 2A). No pH-based model fitted with the final survival of *C. gigas* (Fig. 2C). In contrast, in *O. edulis*, mortalities occurred in all pH conditions throughout the exposure period, and survival dropped to 38% at the lowest pH value (Fig. 2B). The final survival of *O. edulis* fitted with pH according to a segmented regression model with a tipping point at pH_T 6.6, below which survival declined drastically with decreasing pH (Fig. 2C). Above this

tipping point, survival ranged from 93% to 75% and did not correlate with pH (*t*-test, *P*=0.98).

Growth declines with decreasing pH more markedly for *C. gigas*, and shell dissolution occurs at pH 6.6 for both species

At day 41, all biometric parameters declined with decreasing pH for both oyster species (Fig. 3). In *C. gigas*, shell length, growth rate in terms of shell length, and flesh mass decreased significantly as the pH decreased, and reached a tipping point at $\text{pH}_T \sim 7.2$, below which they declined sharply (Fig. 3A,B,F). In contrast, shell mass, total body mass and growth rate calculated from body mass decreased linearly over the entire pH range (Fig. 3C–E). In *O. edulis*, all parameters decreased linearly with pH and showed no tipping point (Fig. 3A–F). Growth rates (calculated from shell length and shell mass) were negative when pH was lower than 6.6 (i.e. critical points) for both species (Fig. 3B,E). For most parameters, slope comparison tests on either side of the tipping point indicated that the

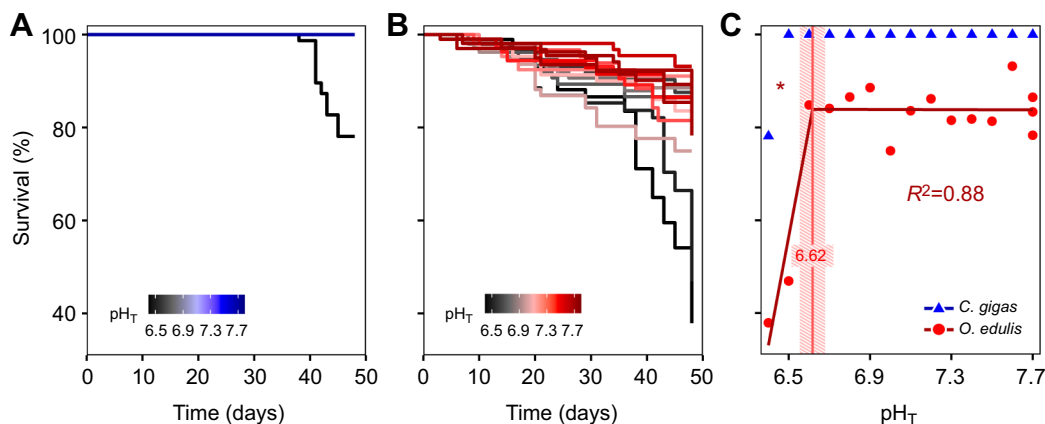


Fig. 2. Survival of oysters of each species as a function of exposure time and pH_T . Kaplan–Meier survival curves of *Crassostrea gigas* (A; log-rank *P*<0.001) and *Ostrea edulis* (B; log-rank *P*<0.001) oysters during 48 days of exposure under 16 pH_T conditions, and final survival of oysters tested against pH_T (C). Each line in A and B represents the survival within a tank, i.e. at a pH_T condition (*n*=1), over 105 individuals per species. In C, each point corresponds to the final survival rate for each species and pH_T condition (*n*=1). Both segmented and linear regression models were tested and the model with the lowest Akaike and Bayesian information criteria and the highest R^2 was selected. The tipping point and 95% confidence interval for survival in *O. edulis* are shown by the vertical red line and striped area; this was not applicable for *C. gigas*. The significance level of the slope is represented using asterisks (**P*<0.05).

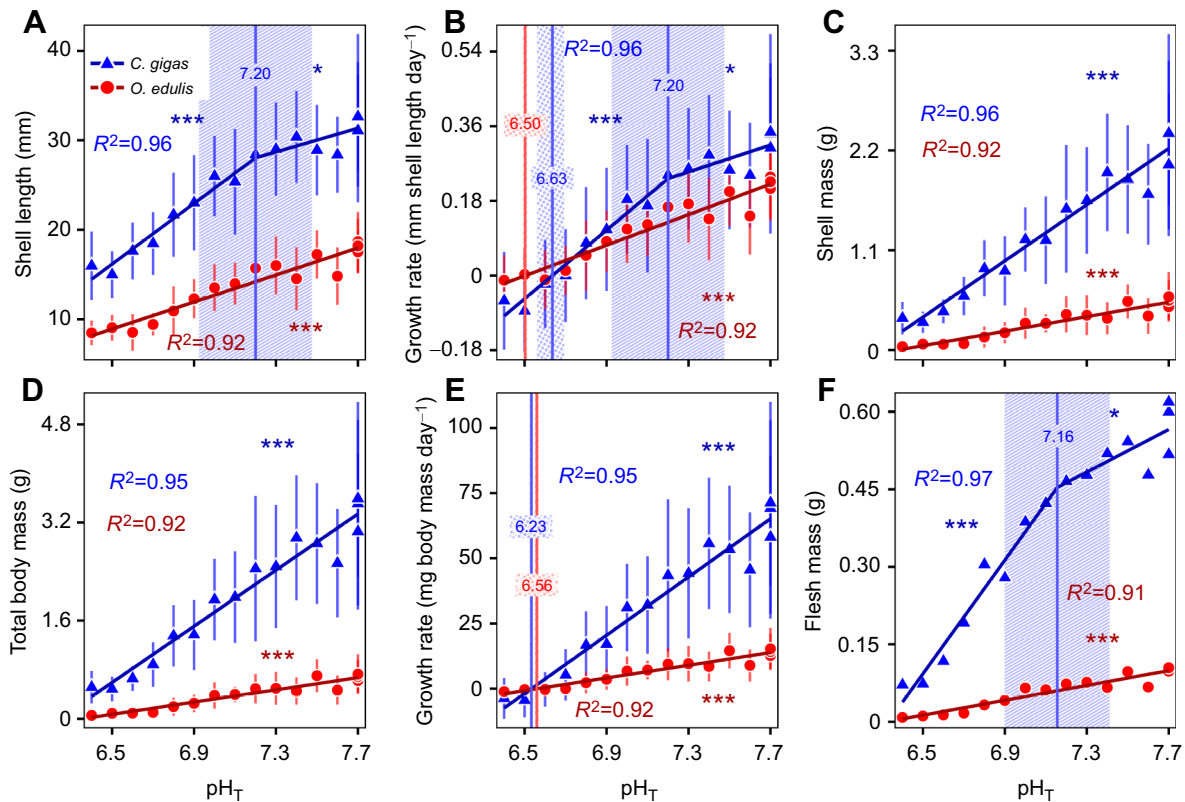


Fig. 3. Final biometric parameters in *C. gigas* and *O. edulis* oysters as a function of pH_T . Shell length (A), growth rate in terms of shell length (B), shell mass (C), total body mass (D), growth rate in terms of total body mass (E) and fresh flesh mass (F) in oysters after 41 days of exposure under 16 pH_T conditions. Data correspond to means \pm s.d. when available ($n=20$ per pH condition and species). Both segmented and linear regression models were tested and the model with the lowest Akaike and Bayesian information criteria and the highest R^2 was selected. The tipping points and 95% confidence intervals are shown by the vertical blue line and striped area for *C. gigas* and by the vertical red line and striped area for *O. edulis*. Critical points and the 95% confidence intervals are shown by the vertical blue line and dotted area for *C. gigas* and by the vertical red line and dotted area for *O. edulis*. The significance level of slopes is represented using asterisks (***) $P < 0.001$, * $P < 0.05$.

reaction norms to pH differed significantly between the two species, and that *C. gigas* generally showed steeper slopes (Table 2).

Shell bleaching increases with decreasing pH for both species

After 20 days of exposure, the mean grayscale value increased with decreasing pH for both species. This indicates that decreasing pH increased shell bleaching (Fig. S3). Shell coloration changed linearly over the pH range in *C. gigas*, while it tipped at pH 6.9 in *O. edulis*, below which it plateaued (t -test, $P=0.58$; Fig. 4). The grayscale values of the shell were similar between the two species at pH_T 7.7 ($F=13.1$, $P=0.07$). A slope comparison test (above the tipping point) indicated that *O. edulis* showed the steepest slope for shell bleaching (Table 2).

Remodelling of membrane lipids occurs in both oyster species in response to decreasing pH, but involves different fatty acids and different tipping points

PCA of membrane fatty acids showed that the first axis (PC1) alone explained 61% and 47% of the total variance in relation to pH for *C. gigas* and *O. edulis*, respectively (Fig. 5A,B). Positively correlated fatty acids mainly consisted of palmitic acid (PA, 16:0), docosahexaenoic acid (DHA, 22:6n-3) and docosapentaenoic acid (DPA, 22:5n-6) in *C. gigas* (Table S1), while they were DHA, DPA and monounsaturated fatty acid (18:1n-7) in *O. edulis* (Table S2). This positively correlated group of fatty acids exhibited tipping

points at $\text{pH}_T \sim 7.0$ for *C. gigas* and $\text{pH}_T \sim 7.5$ for *O. edulis*, below which their contribution to membranes decreased significantly (Fig. 5C). Concomitantly, the main negatively correlated fatty acids consisted of non-methylene-interrupted fatty acid (22:2NMI_{ij}), monounsaturated fatty acid (20:1n-7) and eicosapentaenoic acid (EPA, 20:5n-3) in *C. gigas* (Table S1), while they were dimethyl acetal (18:0DMA) and stearic acid (SA, 18:0) in *O. edulis* (Table S2). This negatively correlated group of fatty acids exhibited tipping points at $\text{pH}_T \sim 7.0$ for *C. gigas* and $\text{pH}_T \sim 7.5$ for *O. edulis*, below which their contribution to membranes increased significantly (Fig. 5D).

Energy reserves are unaffected by decreasing pH for both species

No relationship was found between TAG:ST ratio, total carbohydrate and total protein content and pH_T for both oyster species (Fig. S4), although a segmented regression model was marginally significant for total proteins in *O. edulis* (t -test below tipping point, $P=0.08$; Fig. S4C).

DISCUSSION

Here, we determined and compared the reaction norms to OA in two oyster species living in different habitats: the intertidal Pacific oyster *C. gigas* and the subtidal European flat oyster *O. edulis* exposed in common garden tanks to a seawater pH_T from 7.7 to 6.4 for 48 days. We established the reaction norms of juvenile oysters for survival

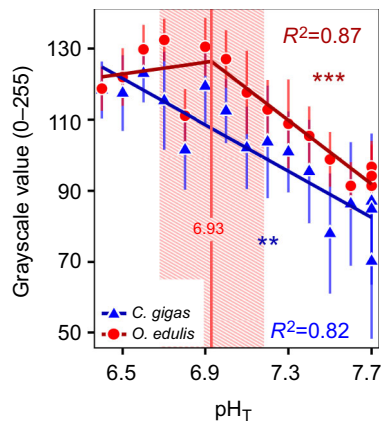


Fig. 4. Shell coloration in *C. gigas* and *O. edulis* oysters as a function of pH_T . Grayscale value corresponds to the shell coloration ranging from 0 (total black) to 255 (total white), after 20 days of exposure under 16 pH_T conditions. Data correspond to means \pm s.d. ($n=15$ per pH condition and species). Both segmented and linear regression models were tested and the model with the lowest Akaike and Bayesian information criteria and the highest R^2 was selected. The tipping points and 95% confidence intervals are shown by the vertical red line and striped area for *O. edulis*. The significance level of slopes is represented using asterisks (*** $P<0.001$, ** $P<0.01$).

rate, biometrics, shell coloration, membrane fatty acids and energy reserves vis-à-vis pH_T . We found that both species showed high plasticity as they were able to survive and grow at extremely low pH_T (>6.6). However, we found that lowering the pH decreased growth performance, increased shell bleaching and induced a major remodelling in membrane lipids. Interestingly, we found several interspecific differences which suggest that the intertidal Pacific oyster has a higher acclimation potential than the subtidal flat oyster to cope with rapid and extreme acidification events.

OA reduces growth-related parameters and causes shell bleaching of oysters

Growth-related parameters decreased as soon as pH declined in both oyster species, probably reflecting the lowering of the calcium carbonate (CaCO_3) saturation state and/or the increase in the metabolic cost of maintaining homeostasis (Beniash et al., 2010; Cyronak et al., 2016). The tipping points observed in *C. gigas* on the biometric parameters in this study are similar to those observed by Lutier et al. (2022), who used the same experimental design. Nevertheless, we obtained significant slopes above tipping points that Lutier et al. (2022) did not observe. This difference in pH responses between the two studies may be associated with differences in the experimental conditions or in the oyster populations used. Indeed, seawater temperature was 19°C in our study compared with 22°C in Lutier et al. (2022). Higher temperature can mitigate the impacts of a pH reduction (Di Poi et al., 2022; Ko et al., 2014). Besides, we used oysters from the same origin as Lutier et al. (2022) but in different years, so their life history and their susceptibility to acidification may have been different (Duarte et al., 2015; Parker et al., 2011; Thor et al., 2018). There are no comparable studies for *O. edulis* in the literature. Overall, the negative impacts on growth-related parameters as soon as pH falls could affect animals' fitness, raising concerns about the future of oyster populations with even small changes in ocean acidity.

In addition, we found that shell bleaching increased with decreasing pH for both species. *Ostrea edulis* exhibited a tipping point at pH_T 6.9 below which the shell colour no longer changed, probably corresponding to a maximal bleaching of the shell. Several studies conducted on oysters and gastropods have also reported shell bleaching at $\text{pH} \sim 7.7-7.8$, which could be attributed to delamination of the periostracum (Avignon et al., 2020; Duquette et al., 2017; Le Moullac et al., 2016; Sezer et al., 2018). Such alteration makes the shell more prone to CaCO_3 dissolution (Peck

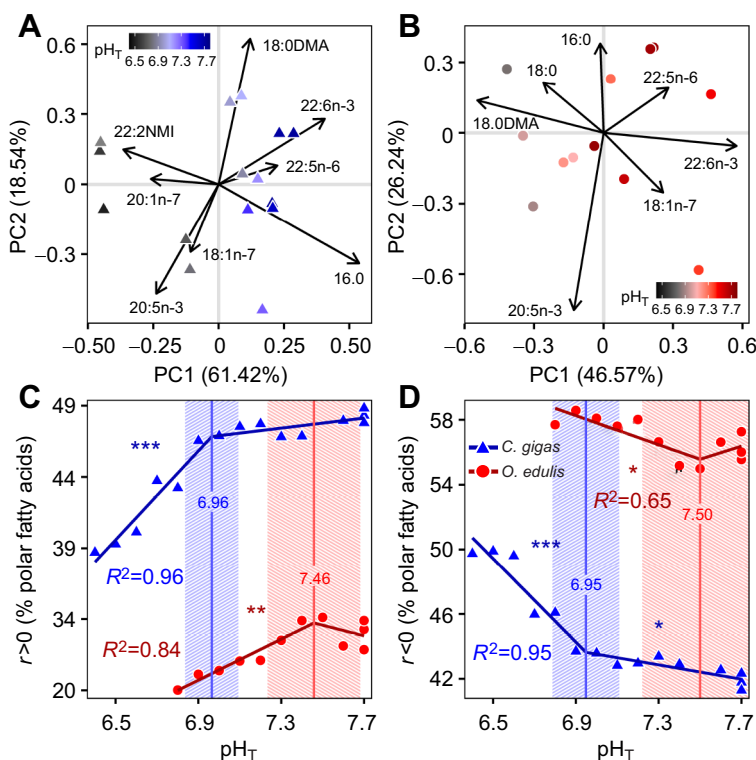


Fig. 5. Membrane fatty acid composition in *C. gigas* and *O. edulis* oysters as a function of pH_T . Principal component analysis of polar fatty acids of *C. gigas* (A) and *O. edulis* (B) after 41 days of exposure under 16 pH_T conditions ($n=10$ oysters pooled per pH condition and species). Arrows represent fatty acids contributing to more than 5% of the first and second principal components (PC1 and PC2). The contributions of fatty acids positively (C) or negatively (D) correlated to PC1 were summed together and tested against pH_T for each oyster species. Both segmented and linear regression models were tested and the model with the lowest Akaike and Bayesian information criteria and the highest R^2 was selected. The tipping points and 95% confidence intervals are shown by the vertical blue line and striped area for *C. gigas* and vertical red line and striped area for *O. edulis*. The significance level of slopes is represented using asterisks (*** $P<0.001$, ** $P<0.01$, * $P<0.05$).

et al., 2016; Tunnicliffe et al., 2009), leading to subsequent changes in biomineral microstructure and shell hardness (Auzoux-Bordenave et al., 2019; Chandra Rajan et al., 2021; Fitzer et al., 2014). Overall, we demonstrate rapid shell alterations due to pH reduction in both species. Compromised shell integrity, resulting from the periostracum delamination, is likely to impair animal fitness and make the oysters more vulnerable to predation and environmental stressors (Waldbusser et al., 2011; Wright et al., 2018).

OA causes a major remodelling of membrane fatty acids

We show for the first time interspecific divergence in the remodelling of membrane fatty acids in response to OA at pH_T 7.0 in *C. gigas* and pH_T 7.5 in *O. edulis*. Remodelling of membrane fatty acids is pivotal to maintaining organism homeostasis in a changing environment (Lee et al., 2018). Similarly, Lutier et al. (2022) reported a major remodelling of fatty acid at pH 7.0 in *C. gigas* juveniles. Overall, very few studies conducted on bivalves have investigated the effects of acidifying conditions on fatty acid composition and there is no such comparison in the literature for *O. edulis*.

Specifically, the level of DHA (22:6n-3) decreased with decreasing pH at the benefit of two molecules related to plasmalogenic phospholipids, which are NMI for *C. gigas* and DMA – a derivative product from plasmalogen transesterification – for *O. edulis*. These results are similar to those obtained in *C. gigas* by Lutier et al. (2022). We hypothesise that oysters' membrane fatty acids were modified in response to low pH to protect cell membranes from oxidative stress while maintaining membrane fluidity. Indeed, DHA is a long-chain polyunsaturated fatty acid (PUFA) that is particularly susceptible to peroxidation (Munro and Blier, 2012), whereas NMI and plasmalogens can act as scavengers of reactive oxygen species (Barnathan, 2009; Kraffe et al., 2004; Leray et al., 2002; Munro and Blier, 2012). In addition, NMI and plasmalogens may contribute to maintaining membrane fluidity and ion exchange between intracellular and extracellular compartments (Munro and Blier, 2012). Here, we show that the two oyster species use the same biochemical machinery to cope with low pH, but their tipping points vary markedly, suggesting different strategies.

Oysters are tolerant to corrosive water

Both oyster species survive and grow at pH levels as low as 6.6 while seawater was undersaturated in calcite and aragonite ($\Omega_C=0.2$ and $\Omega_A=0.1$). Several studies have reported the ability of molluscs to calcify and grow in corrosive seawater, e.g. the mussels *Mytilus edulis* in Berge et al. (2006) and *Bathymodiolus brevior* in Tunnicliffe et al. (2009), and the limpet *Patella caerulea* in Rodolfo-Metalpa et al. (2011).

Note, however, that the oysters were fed *ad libitum* and their energy reserves were unaffected by a pH decrease. It is likely that food availability allowed oysters to cope with acidification while maintaining positive growth without depleting reserves. The effects of acidification on growth and energy may be more pronounced under limiting food conditions (Hettinger et al., 2013; Sanders et al., 2013; Thomsen et al., 2013). We may have underestimated the impacts of OA in our study and it would be interesting to obtain reaction norms under different food levels.

However, at $\text{pH}_T > 6.6$, oyster shells were smaller than at the onset of the experiment, reflecting a net dissolution of the shell in both species. This coincides with a marked increase in mortality in *O. edulis*, suggesting death by shell dissolution (Green et al., 2009). At this pH_T , *C. gigas* showed no mortality and reserves were not depleted. We hypothesise that *C. gigas* went through metabolic

depression to cope with such an extreme acidification event. Indeed, organisms can shift to metabolic rate depression enabling them to delay the onset of homeostatic disturbances incompatible with survival (Guppy and Withers, 1999; Sokolova, 2021). This time-limited survival strategy was previously suggested in Lutier et al. (2022) in juvenile *C. gigas* exposed to extremely acidic waters thanks to additional respiration and calcification data. The absence of data on the state of reserves at this pH in *O. edulis* does not allow us to draw such a conclusion. Although both oyster species are tolerant to OA, they deploy different short-term survival strategies in highly corrosive waters, with *C. gigas* showing the greatest acclimation potential.

Oyster species exhibit different physiological trade-offs to cope with OA

Reaction norms differed markedly between the two oyster species. Acidification has a greater effect on the growth of *C. gigas*, as shown by the steeper regression slopes, compared with *O. edulis*, but its survival is better. Under acidified conditions, *C. gigas* may allocate a greater proportion of energy to maintenance processes to stay alive at the expense of growth than *O. edulis*. Such trade-offs between growth and survival under stressful conditions were previously suggested in several studies (Gazeau et al., 2013; Stumpp et al., 2011; Thomsen and Melzner, 2010). In addition, the marked decrease in growth in *C. gigas* in response to low pH may reflect shell dissolution that could compensate for internal acidosis by increasing bicarbonate ions in tissues and extracellular fluids (Michaelidis et al., 2005). Conversely, *O. edulis* may allocate energy towards growth at the expense of homeostasis. A full energy budget is necessary to further investigate the physiological trade-offs in response to pH.

These different strategies exhibited by the two oyster species towards OA can be explained by their respective habitats. Intertidal organisms that live in highly variable environments are likely to be more tolerant to pH fluctuation than those living in the more stable subtidal zone (Melzner et al., 2009; Vargas et al., 2017, 2022). Comparative studies have suggested that the intertidal *C. gigas* could even outcompete the subtidal *O. edulis* under fluctuating environmental conditions (Gilson et al., 2021; Green et al., 2017; Stechele et al., 2022). Moreover, the different strategies in reproduction associated with somatic allocation between the two species may help explain their response to OA (Stechele et al., 2022). Indeed, the flat oyster seems more susceptible to unfavourable environmental conditions during the brooding period, while the Pacific oyster's high-energy investment in reproduction and its capacity for massive spawning are beneficial in changing environments. Particularly with regard to seawater acidification, Bamber (1990) established the reaction norms to pH in *C. gigas* and *O. edulis* after a 30 day exposure and reported the highest sensitivity of *O. edulis*, although the pH gradient and the experimental procedure for acidifying the water (adding sulphuric acid) may be questionable. Overall, our results show that the intertidal Pacific oyster may have a higher acclimation potential than the subtidal flat oyster to cope with rapid and extreme OA events.

Nevertheless, the conclusions must be nuanced. Firstly, the two species, at the same age, were not the same size and probably did not have the same growth potential. Generally, flat oysters have a lower filtration rate, slower growth, smaller ultimate size and more limited energy storage than the Pacific oyster (Stechele et al., 2022), which may influence their tolerance to pH. The experiment was also conducted without a tidal regime for *C. gigas*, which may have led to an underestimation of OA effects in intertidal oyster species (Scanes et al., 2017).

Conclusion

Our study provides important data about the plasticity capacity and tolerance thresholds of two oyster species living in different habitats to future global changes. However, further work integrating several oyster populations and genetic lines under different food regimes and temperatures is needed to fully characterise species-specific reaction norms. We emphasise the need for considering habitat-specific variability of pH/ P_{CO_2} based on *in situ* observations to design more realistic experiments.

Acknowledgements

We thank the Ifremer staff from Argenton and Bouin for animal production and maintenance. We are particularly grateful to Moussa Diagne for phytoplankton production, Matthias Huber, Isabelle Queau and Jacqueline Le Grand for zootechnical support, and Claudie Quere and Valerian Le Roy for biochemical analyses (Ifremer, LEMAR). We thank Vincent Ouisse and Elodie Foucault (Ifremer-Laboratoire Environnement Ressources Languedoc-Roussillon) for total alkalinity analyses. This work is part of the PhD thesis of C.C. (Caillon, 2023).

Competing interests

The authors declare no competing or financial interests.

Author contributions

Conceptualization: C.C., F.P., M.L., C.D.; Methodology: C.C., F.P., M.L., C.D.; Formal analysis: C.C., F.P., M.L., C.D.; Investigation: C.C., F.P., C.D.; Data curation: C.C.; Resources: F.P., C.D.; Writing - original draft: C.C., C.D.; Writing - review & editing: F.P., M.L.; Visualization: C.C., M.L., F.P., C.D.; Supervision: F.P., C.D.; Funding acquisition: F.P.

Funding

The study was financially supported by the Ocean Acidification Program of the Fondation pour la Recherche sur la Biodiversité (FRB, www.fondationbiodiversite.fr) and the French Ministère de l'Écologie, du Développement Durable et de l'Énergie.

Data availability

Raw data supporting the findings of this study are publicly available at the SEANOE DIGITAL Repository: <https://doi.org/10.17882/95793>.

References

- Auzoux-Bordenave, S., Wessel, N., Badou, A., Martin, S., M'zoudi, S., Avignon, S., Roussel, S., Huchette, S. and Dubois, P. (2019). Ocean acidification impacts growth and shell mineralization in juvenile abalone (*Haliotis tuberculata*). *Mar. Biol.* **167**, 11. doi:10.1007/s00227-019-3623-0
- Avignon, S., Auzoux-Bordenave, S., Martin, S., Dubois, P., Badou, A., Coheleach, M., Richard, N., Di Giglio, S., Malet, L., Servili, A. et al. (2020). An integrated investigation of the effects of ocean acidification on adult abalone (*Haliotis tuberculata*). *ICES J. Mar. Sci.* **77**, 757-772. doi:10.1093/icesjms/fsz257
- Bamber, R. N. (1990). The effects of acidic seawater on three species of lamellibranch mollusc. *J. Exp. Mar. Biol. Ecol.* **143**, 181-191. doi:10.1016/0022-0981(90)90069-0
- Barnathan, G. (2009). Non-methylene-interrupted fatty acids from marine invertebrates: occurrence, characterization and biological properties. *Biochimie* **91**, 671-678. doi:10.1016/j.biochi.2009.03.020
- Bayne, B. L. (2017). *Biology of Oysters*. Academic Press.
- Beniash, E., Ivanina, A., Lieb, N. S., Kurochkin, I. and Sokolova, I. M. (2010). Elevated level of carbon dioxide affects metabolism and shell formation in oysters *Crassostrea virginica*. *Mar. Ecol. Prog. Ser.* **419**, 95-108. doi:10.3354/meps08841
- Berge, J. A., Bjerkeng, B., Pettersen, O., Schaanning, M. T. and Øxnevad, S. (2006). Effects of increased sea water concentrations of CO₂ on growth of the bivalve *Mytilus edulis* L. *Chemosphere* **62**, 681-687. doi:10.1016/j.chemosphere.2005.04.111
- Burnett, L. E. (1988). Physiological responses to air exposure: acid-base balance and the role of branchial water stores. *Am. Zool.* **28**, 125-135. doi:10.1093/icb/28.1.125
- Cai, W.-J., Hu, X., Huang, W.-J., Murrell, M. C., Lehrter, J. C., Lohrenz, S. E., Chou, W.-C., Zhai, W., Hollibaugh, J. T., Wang, Y. et al. (2011). Acidification of subsurface coastal waters enhanced by eutrophication. *Nat. Geosci.* **4**, 766-770. doi:10.1038/ngeo1297
- Caillon C. (2023). Plasticité phénotypique des huîtres face à l'acidification et au réchauffement des océans sous différentes contraintes environnementales. PhD thesis, Université de Bretagne Occidentale.
- Caldeira, K. and Wickett, M. E. (2003). Anthropogenic carbon and ocean pH. *Nature* **425**, 365-365. doi:10.1038/425365a
- Chandra Rajan, K., Meng, Y., Yu, Z., Roberts, S. B. and Vengatesen, T. (2021). Oyster biomineralization under ocean acidification: from genes to shell. *Glob. Change Biol.* **27**, 3779-3797. doi:10.1111/gcb.15675
- Chevin, L.-M. and Hoffmann, A. A. (2017). Evolution of phenotypic plasticity in extreme environments. *Philos. Trans. R. Soc. B: Biol. Sci.* **372**, 20160138. doi:10.1098/rstb.2016.0138
- Comeau, S., Edmunds, P. J., Spindel, N. B. and Carpenter, R. C. (2013). The responses of eight coral reef calcifiers to increasing partial pressure of CO₂ do not exhibit a tipping point. *Limnol. Oceanogr.* **58**, 388-398. doi:10.4319/lo.2013.58.1.0388
- Couturier, L. I. E., Michel, L. N., Amaro, T., Budge, S. M., Da Costa, E., De Troch, M., Di Dato, V., Fink, P., Giraldo, C., Le Grand, F. et al. (2020). State of art and best practices for fatty acid analysis in aquatic sciences. *ICES J. Mar. Sci.* **77**, 2375-2395. doi:10.1093/icesjms/fsaa121
- Cyronak, T., Schulz, K. G. and Jokiel, P. L. (2016). The Omega myth: what really drives lower calcification rates in an acidifying ocean. *ICES J. Mar. Sci.* **73**, 558-562. doi:10.1093/icesjms/fsv075
- Dickson, A. G., Sabine, C. L., Christian, J. R. and Barger, C. P. and North Pacific Marine Science Organization. eds. (2007). *Guide to Best Practices for Ocean CO₂ Measurements*. Sidney, BC: North Pacific Marine Science Organization.
- Di Poi, C., Brodu, N., Gazeau, F. and Pernet, F. (2022). Life-history traits in the Pacific oyster *Crassostrea gigas* are robust to ocean acidification under two thermal regimes. *ICES J. Mar. Sci.* **79**, 2614-2629. doi:10.1093/icesjms/fsac195
- Dorey, N., Lançon, P., Thorndyke, M. and Dupont, S. (2013). Assessing physiological tipping point of sea urchin larvae exposed to a broad range of pH. *Glob. Change Biol.* **19**, 3355-3367. doi:10.1111/gcb.12276
- Duarte, C., Navarro, J. M., Acuña, K., Torres, R., Manríquez, P. H., Lardies, M. A., Vargas, C. A., Lagos, N. A. and Aguilera, V. (2015). Intraspecific variability in the response of the edible mussel *Mytilus chilensis* (Hupe) to ocean acidification. *Estuaries Coast.* **38**, 590-598. doi:10.1007/s12237-014-9845-y
- Dubois, M., Gilles, K. A., Hamilton, J. K., Rebers, P. A. and Smith, F. (1956). Colorimetric method for determination of sugars and related substances. *Anal. Chem.* **28**, 350-356. doi:10.1021/ac60111a017
- Duquette, A., McClintock, J. B., Amsler, C. D., Pérez-Huerta, A., Milazzo, M. and Hall-Spencer, J. M. (2017). Effects of ocean acidification on the shells of four Mediterranean gastropod species near a CO₂ seep. *Mar. Pollut. Bull.* **124**, 917-928. doi:10.1016/j.marpolbul.2017.08.007
- Feely, R. A., Sabine, C. L., Hernandez-Ayon, J. M., Ianson, D. and Hales, B. (2008). Evidence for upwelling of corrosive "acidified" water onto the continental shelf. *Science* **320**, 1490-1492. doi:10.1126/science.1155676
- Fitzer, S. C., Cusack, M., Phoenix, V. R. and Kamenos, N. A. (2014). Ocean acidification reduces the crystallographic control in juvenile mussel shells. *J. Struct. Biol.* **188**, 39-45. doi:10.1016/j.jsb.2014.08.007
- Fraser, A. J. (1989). Triacylglycerol content as a condition index for fish, bivalve, and crustacean larvae. *Can. J. Fish. Aquat. Sci.* **46**, 1868-1873. doi:10.1139/f89-235
- Gazeau, F., Parker, L. M., Comeau, S., Gattuso, J.-P., O'Connor, W. A., Martin, S., Pörtner, H.-O. and Ross, P. M. (2013). Impacts of ocean acidification on marine shelled molluscs. *Mar. Biol.* **160**, 2207-2245. doi:10.1007/s00227-013-2219-3
- Gilson, A. R., Coughlan, N. E., Dick, J. T. A. and Kregting, L. (2021). Marine heat waves differentially affect functioning of native (*Ostrea edulis*) and invasive (*Crassostrea [Magallana] gigas*) oysters in tidal pools. *Mar. Environ. Res.* **172**, 105497. doi:10.1016/j.marenvres.2021.105497
- Gray, M. W., Chaparro, O., Huebert, K. B., O'Neill, S. P., Couture, T., Moreira, A. and Brady, D. C. (2019). Life history traits conferring larval resistance against ocean acidification: the case of brooding oysters of the genus *Ostrea*. *J. Shellfish Res.* **38**, 751-761. doi:10.2983/035.038.0326
- Green, M. A., Waldbusser, G. G., Reilly, S. L., Emerson, K. and O'Donnell, S. (2009). Death by dissolution: sediment saturation state as a mortality factor for juvenile bivalves. *Limnol. Oceanogr.* **54**, 1037-1047. doi:10.4319/lo.2009.54.4.1037
- Green, D. S., Christie, H., Pratt, N., Boots, B., Godbold, J. A., Solan, M. and Hauton, C. (2017). Competitive interactions moderate the effects of elevated temperature and atmospheric CO₂ on the health and functioning of oysters. *Mar. Ecol. Prog. Ser.* **582**, 93-103. doi:10.3354/meps12344
- Guppy, M. and Withers, P. (1999). Metabolic depression in animals: physiological perspectives and biochemical generalizations. *Biol. Rev.* **74**, 1-40. doi:10.1111/j.1469-185X.1999.tb00180.x
- Hettinger, A., Sanford, E., Hill, T. M., Hosfelt, J. D., Russell, A. D. and Gaylord, B. (2013). The influence of food supply on the response of Olympia oyster larvae to ocean acidification. *Biogeosciences* **10**, 6629-6638. doi:10.5194/bg-10-6629-2013
- Hofmann, G. E., Smith, J. E., Johnson, K. S., Send, U., Levin, L. A., Micheli, F., Paytan, A., Price, N. N., Peterson, B., Takeshita, Y. et al. (2011). High-frequency dynamics of ocean pH: a multi-ecosystem comparison. *PLoS One* **6**, e28983. doi:10.1371/journal.pone.0028983

- Hulbert, A. J. (2003). Life, death and membrane bilayers. *J. Exp. Biol.* **206**, 2303-2311. doi:10.1242/jeb.00399
- IPCC (2022). Climate Change 2022: Impacts, Adaptation, and Vulnerability. *Contribution of Working Group II to the Sixth Assessment Report of the Intergovernmental Panel on Climate Change* (ed. H.-O. Pörtner, D. C. Roberts, M. Tignor, E. S. Poloczanska, K. Mintenbeck, A. Alegria, M. Craig, S. Langsdorf, S. Löschke, V. Möller, A. Okem, B. Rama), p. 3056. Cambridge University Press.
- Kaplan, E. L. and Meier, P. (1958). Nonparametric estimation from incomplete observations. *J. Am. Stat. Assoc.* **53**, 457-481. doi:10.1080/01621459.1958.10501452
- Ko, G. W. K., Dineshram, R., Campanati, C., Chan, V. B. S., Havenhand, J. and Thiagarajan, V. (2014). Interactive effects of ocean acidification, elevated temperature, and reduced salinity on early-life stages of the Pacific oyster. *Environ. Sci. Technol.* **48**, 10079-10088. doi:10.1021/es501611u
- Kraffe, E., Soudant, P. and Marty, Y. (2004). Fatty acids of serine, ethanolamine, and choline plasmalogens in some marine bivalves. *Lipids* **39**, 59-66. doi:10.1007/s11745-004-1202-x
- Laing, I., Walker, P. and Areal, F. (2006). Return of the native – is European oyster (*Ostrea edulis*) stock restoration in the UK feasible? *Aquat. Living Resour.* **19**, 283-287. doi:10.1051/alr:2006029
- Le Moullac, G., Soyez, C., Vidal-Dupiol, J., Belliard, C., Fievet, J., Sham-Koua, M., Lo-Yat, A., Saulnier, D., Gaertner-Mazouni, N. and Gueguen, Y. (2016). Impact of pCO₂ on the energy, reproduction and growth of the shell of the pearl oyster *Pinctada margaritifera*. *Estuar Coast Shelf Sci* **182**, 274-282. doi:10.1016/j.ecss.2016.03.011
- Lee, M.-C., Park, J. C. and Lee, J.-S. (2018). Effects of environmental stressors on lipid metabolism in aquatic invertebrates. *Aquat. Toxicol.* **200**, 83-92. doi:10.1016/j.aquatox.2018.04.016
- Leeuwis, R. H. J. and Gamperl, A. K. (2022). Adaptations and plastic phenotypic responses of marine animals to the environmental challenges of the high intertidal zone. *Oceanogr. Mar. Biol. Annu. Rev.* **60**, 625-680. doi:10.1201/9781003288602-13
- Leray, C., Cazenave, J.-P. and Gachet, C. (2002). Platelet phospholipids are differentially protected against oxidative degradation by plasmalogens. *Lipids* **37**, 285-290. doi:10.1007/s11745-002-0892-4
- Leung, J. Y. S., Connell, S. D., Nagelkerken, I. and Russell, B. D. (2017). Impacts of near-future ocean acidification and warming on the shell mechanical and geochemical properties of gastropods from intertidal to subtidal zones. *Environ. Sci. Technol.* **51**, 12097-12103. doi:10.1021/acs.est.7b02359
- Lowry, O. H., Rosebrough, N. J., Farr, A. L. and Randall, R. J. (1951). Protein measurement with the Folin phenol reagent. *J. Biol. Chem.* **193**, 265-275. doi:10.1016/S0021-9258(19)52451-6
- Lutier, M., Di Poi, C., Gazeau, F., Appolis, A., Le Luyet, J. and Pernet, F. (2022). Revisiting tolerance to ocean acidification: insights from a new framework combining physiological and molecular tipping points of Pacific oyster. *Glob. Change Biol.* **28**, 3333-3348. doi:10.1111/gcb.16101
- Maneiro, V., Santos, Y., Pazos, A. J., Silva, A., Torres-Corral, Y., Sánchez, J. L. and Pérez-Parallé, M. L. (2020). Effects of food ration, water flow rate and bacteriological levels of broodstock on the reproductive conditioning of the European flat oyster (*Ostrea edulis*, Linnaeus 1758). *Aquac. Rep.* **18**, 100412. doi:10.1016/j.aqrep.2020.100412
- Melzner, F., Gutowska, M. A., Langenbuch, M., Dupont, S., Lucassen, M., Thorndyke, M. C., Bleich, M. and Pörtner, H.-O. (2009). Physiological basis for high CO₂ tolerance in marine ectothermic animals: pre-adaptation through lifestyle and ontogeny? *Biogeosciences* **6**, 2313-2331. doi:10.5194/bg-6-2313-2009
- Michaelidis, B., Haas, D. and Grieshaber, M. K. (2005). Extracellular and intracellular acid-base status with regard to the energy metabolism in the oyster *Crassostrea gigas* during exposure to air. *Physiol. Biochem. Zool.* **78**, 373-383. doi:10.1086/430223
- Munro, D. and Blier, P. U. (2012). The extreme longevity of *Arctica islandica* is associated with increased peroxidation resistance in mitochondrial membranes. *Aging Cell* **11**, 845-855. doi:10.1111/j.1474-9726.2012.00847.x
- Orr, J. C., Fabry, V. J., Aumont, O., Bopp, L., Doney, S. C., Feely, R. A., Gnanadesikan, A., Gruber, N., Ishida, A., Joos, F. et al. (2005). Anthropogenic ocean acidification over the twenty-first century and its impact on calcifying organisms. *Nature* **437**, 681-686. doi:10.1038/nature04095
- Parker, L. M., Ross, P. M. and O'Connor, W. A. (2010). Comparing the effect of elevated pCO₂ and temperature on the fertilization and early development of two species of oysters. *Mar. Biol.* **157**, 2435-2452. doi:10.1007/s00227-010-1508-3
- Parker, L. M., Ross, P. M. and O'Connor, W. A. (2011). Populations of the Sydney rock oyster, *Saccostrea glomerata*, vary in response to ocean acidification. *Mar. Biol.* **158**, 689-697. doi:10.1007/s00227-010-1592-4
- Peck, V. L., Tarling, G. A., Manno, C., Harper, E. M. and Tynan, E. (2016). Outer organic layer and internal repair mechanism protects pteropod *Limacina helicina* from ocean acidification. *Deep Sea Res. II: Top. Stud. Oceanogr.* **127**, 41-52. doi:10.1016/j.dsr2.2015.12.005
- Petton, B., Boudry, P., Alunno-Bruscia, M. and Pernet, F. (2015). Factors influencing disease-induced mortality of Pacific oysters *Crassostrea gigas*. *Aquacult. Environ. Interact.* **6**, 205-222. doi:10.3354/aei00125
- Pogoda, B. (2019). Current status of European oyster decline and restoration in Germany. *Humanities* **8**, 9. doi:10.3390/h8010009
- Provoost, P., Van Heuven, S., Soetaert, K., Laane, R. W. P. M. and Middelburg, J. J. (2010). Seasonal and long-term changes in pH in the Dutch coastal zone. *Biogeosciences* **7**, 3869-3878. doi:10.5194/bg-7-3869-2010
- Rodolfo-Metalpa, R., Houlbrèque, F., Tambutté, É., Boisson, F., Baggini, C., Patti, F. P., Jeffree, R., Fine, M., Foggio, A., Gattuso, J.-P. et al. (2011). Coral and mollusc resistance to ocean acidification adversely affected by warming. *Nat. Clim. Change* **1**, 308-312. doi:10.1038/nclimate1200
- Sanders, M. B., Bean, T. P., Hutchinson, T. H. and Quesne, W. J. F. L. (2013). Juvenile king scallop, *Pecten maximus*, is potentially tolerant to low levels of ocean acidification when food is unrestricted. *PLoS One* **8**, e74118. doi:10.1371/journal.pone.0074118
- Scanes, E., Parker, L. M., O'Connor, W. A., Stapp, L. S. and Ross, P. M. (2017). Intertidal oysters reach their physiological limit in a future high-CO₂ world. *J. Exp. Biol.* **220**, 765-774. doi:10.1242/jeb.151365
- Scheffer, M. (2010). Foreseeing tipping points. *Nature* **467**, 411-412. doi:10.1038/467411a
- Sezer, N., Kılıç, Ö., Metian, M., Belivermiş, M. and Belivermiş, M. (2018). Effects of ocean acidification on ¹⁰⁹Cd, ⁵⁷Co, and ¹³⁴Cs bioconcentration by the European oyster (*Ostrea edulis*): biokinetics and tissue-to-subcellular partitioning. *J. Environ. Radioact.* **192**, 376-384. doi:10.1016/j.jenvrad.2018.07.011
- Sokolova, I. M. (2013). Energy-limited tolerance to stress as a conceptual framework to integrate the effects of multiple stressors. *Integr. Comp. Biol.* **53**, 597-608. doi:10.1093/icb/ict028
- Sokolova, I. M. (2021). Bioenergetics in environmental adaptation and stress tolerance of aquatic ectotherms: linking physiology and ecology in a multi-stressor landscape. *J. Exp. Biol.* **224**, jeb236802. doi:10.1242/jeb.236802
- Stechele, B., Maar, M., Wijsman, J., Van Der Zande, D., Degraer, S., Bossier, P. and Nevejan, N. (2022). Comparing life history traits and tolerance to changing environments of two oyster species (*Ostrea edulis* and *Crassostrea gigas*) through Dynamic Energy Budget theory. *Conserv. Physiol.* **10**, coac034. doi:10.1093/conphys/coac034
- Stumpff, M., Wren, J., Melzner, F., Thorndyke, M. C. and Dupont, S. T. (2011). CO₂ induced seawater acidification impacts sea urchin larval development I: elevated metabolic rates decrease scope for growth and induce developmental delay. *Comp. Biochem. Physiol. A: Mol. Integr. Physiol.* **160**, 331-340. doi:10.1016/j.cbpa.2011.06.022
- Thomsen, J. and Melzner, F. (2010). Moderate seawater acidification does not elicit long-term metabolic depression in the blue mussel *Mytilus edulis*. *Mar. Biol.* **157**, 2667-2676. doi:10.1007/s00227-010-1527-0
- Thomsen, J., Casties, I., Pansch, C., Körtzinger, A. and Melzner, F. (2013). Food availability outweighs ocean acidification effects in juvenile *Mytilus edulis*: laboratory and field experiments. *Glob. Change Biol.* **19**, 1017-1027. doi:10.1111/gcb.12109
- Thomsen, J., Stapp, L. S., Haynert, K., Schade, H., Danelli, M., Lannig, G., Wegner, K. M. and Melzner, F. (2017). Naturally acidified habitat selects for ocean acidification-tolerant mussels. *Sci. Adv.* **3**, e1602411. doi:10.1126/sciadv.1602411
- Thor, P., Bailey, A., Dupont, S., Calosi, P., Søreide, J. E., De Wit, P., Guscetti, E., Loubet-Sartrou, L., Deichmann, I. M., Candee, M. M. et al. (2018). Contrasting physiological responses to future ocean acidification among Arctic copepod populations. *Glob. Change Biol.* **24**, e365-e377. doi:10.1111/gcb.13870
- Tunnicliffe, V., Davies, K. T. A., Butterfield, D. A., Embley, R. W., Rose, J. M. and Chadwick, W. W., Jr. (2009). Survival of mussels in extremely acidic waters on a submarine volcano. *Nat. Geosci.* **2**, 344-348. doi:10.1038/ngeo500
- Vargas, C. A., Lagos, N. A., Lardies, M. A., Duarte, C., Manríquez, P. H., Aguilera, V. M., Broitman, B., Widdicombe, S. and Dupont, S. (2017). Species-specific responses to ocean acidification should account for local adaptation and adaptive plasticity. *Nat. Ecol. Evol.* **1**, 84. doi:10.1038/s41559-017-0084
- Vargas, C. A., Cuevas, L. A., Broitman, B. R., San Martín, V. A., Lagos, N. A., Gaitán-Espitia, J. D. and Dupont, S. (2022). Upper environmental pCO₂ drives sensitivity to ocean acidification in marine invertebrates. *Nature Climate Change* **12**, 200-207. doi:10.1038/s41558-021-01269-2
- Ventura, A., Schulz, S. and Dupont, S. (2016). Maintained larval growth in mussel larvae exposed to acidified under-saturated seawater. *Sci. Rep.* **6**, 23728. doi:10.1038/srep23728
- Waldbusser, G. G., Voigt, E. P., Bergschneider, H., Green, M. A. and Newell, R. I. E. (2011). Biocalcification in the Eastern oyster (*Crassostrea virginica*) in relation to long-term trends in Chesapeake Bay pH. *Estuaries Coast.* **34**, 221-231. doi:10.1007/s12237-010-9307-0
- Waldbusser, G. G., Hales, B., Langdon, C. J., Haley, B. A., Schrader, P., Brunner, E. L., Gray, M. W., Miller, C. A. and Gimenez, I. (2015). Saturation-state sensitivity of marine bivalve larvae to ocean acidification. *Nat. Clim. Change* **5**, 273-280. doi:10.1038/nclimate2479
- Wood, S. N. (2001). Minimizing model fitting objectives that contain spurious local minima by bootstrap restarting. *Biometrics* **57**, 240-244. doi:10.1111/j.0006-341X.2001.00240.x

- Wright, J. M., Parker, L. M., O'connor, W. A., Scanes, E. and Ross, P. M. (2018).** Ocean acidification affects both the predator and prey to alter interactions between the oyster *Crassostrea gigas* (Thunberg, 1793) and the whelk *Tenguella marginalba* (Blainville, 1832). *Mar. Biol.* **165**, 46. doi:10.1007/s00227-018-3302-6
- Zwerschke, N., Kochmann, J., Ashton, E. C., Crowe, T. P., Roberts, D. and O'connor, N. E. (2018).** Co-occurrence of native *Ostrea edulis* and non-native *Crassostrea gigas* revealed by monitoring of intertidal oyster populations. *J. Mar. Biol. Assoc. U. K.* **98**, 2029-2038. doi:10.1017/S0025315417001448